

Behavior Subtraction

Pierre-Marc Jodoin, *Member, IEEE*, Venkatesh Saligrama, *Senior Member, IEEE*,
and Janusz Konrad, *Fellow, IEEE*

Abstract—Background subtraction has been a driving engine for many computer vision and video analytics tasks. Although its many variants exist, they all share the underlying assumption that photometric scene properties are either static or exhibit temporal stationarity. While this works in some applications, the model fails when one is interested in discovering *changes in scene dynamics* rather than those in a static background; detection of unusual pedestrian and motor traffic patterns is but one example. We propose a new model and computational framework that address this failure by considering stationary scene dynamics as a “background” with which observed scene dynamics are compared. Central to our approach is the concept of an *event*, that we define as short-term scene dynamics captured over a time window at a specific spatial location in the camera field of view. We compute events by time-aggregating motion labels, obtained by background subtraction, as well as object descriptors (e.g., object size). Subsequently, we characterize events probabilistically, but use a low-memory, low-complexity surrogates in practical implementation. Using these surrogates amounts to *behavior subtraction*, a new algorithm with some surprising properties. As demonstrated here, behavior subtraction is an effective tool in anomaly detection and localization. It is resilient to spurious background motion, such as one due to camera jitter, and is content-blind, i.e., it works equally well on humans, cars, animals, and other objects in both uncluttered and highly-cluttered scenes. Clearly, treating video as a collection of events rather than colored pixels opens new possibilities for video analytics.

Index Terms—Video analysis, activity analysis, anomaly detection, behavior modeling, video surveillance.

I. INTRODUCTION

MANY computer vision and video analytics algorithms rely on background subtraction as the engine of choice for detecting areas of interest (change). Although a number of models have been developed for background subtraction, from single Gaussian [?] and mixture of Gaussians [?] to non-parametric kernel methods [?]¹, they all share the underlying assumption that photometric scene properties (e.g., luminance, color) are either static or exhibit temporal stationarity. The static background assumption works quite well for some applications, e.g., indoor scenes under constant illumination, while the temporally-stationary background assumption is needed in other cases, such as outdoor scenes with natural phenomena (e.g., fluttering leaves). However, both models fail if one is interested in discovering *changes in scene dynamics* rather than those taking place in a static background. Examples of

such scenario are: detection of unusual motor traffic patterns (e.g., too fast or too slow), detection of a moving group of individuals where a single walking person is expected, detection of a moving object against shimmering or turbulent water surface (background motion). Although each of these challenges can be addressed by a custom-built method, e.g., explicitly estimating object trajectories or discovering the number of moving objects, there is no approach to-date that can address *all* such scenarios in a single framework.

In order to address this challenge, instead of searching for photometric deviations in time, one should look for dynamic deviations in time. To date, the problem has been attacked primarily by analyzing two-dimensional motion paths resulting from tracking objects or people [?], [?], [?], [?], [?]. Usually, reference motion paths are computed from a training video sequence first. Then, the same tracking algorithm is applied to an observed video sequence, and the resulting paths are compared with the reference motion paths. Unfortunately, such methods require many computing stages, from low-level detection to high-level inferencing [?], and often result in failure due to multiple, sequential steps.

In this paper, we propose a new model and computational framework that extend background subtraction to, what we call, *behavior subtraction* [?], while at the same time addressing deficiencies of motion-path-based algorithms. Whereas in background subtraction static or stationary photometric properties (e.g., luminance or color) are assumed as the background image, we propose to use stationary scene dynamics as a “background” activity with which observed scene dynamics are compared. The approach we propose requires neither computation of motion nor object tracking, and, as such, is less prone to failure. Central to our approach is the concept of an *event*, that we define as short-term scene dynamics captured over a time window at a specific spatial location in the camera field of view. We compute events by time-aggregating motion labels and/or suitable object descriptors (e.g., size). Subsequently, we characterize events probabilistically as random variables that are independent and identically distributed (*iid*) in time. Since the estimation of a probability density function (PDF) at each location is both memory- and CPU-intensive, in practical implementation we resort to a low-memory, low-complexity surrogate. Using such a surrogate amounts to behavior subtraction, a new algorithm with some surprising properties. As we demonstrate experimentally, behavior subtraction is an effective tool in anomaly detection, including localization, but can also serve as motion detector very resilient to spurious background motion, e.g., resulting from camera jitter. Furthermore, it is content-blind, i.e., applicable to humans, cars, animals, and other objects in both uncluttered and highly-cluttered scenes.

Manuscript submitted in August 2009

P.-M. Jodoin is with the Université de Sherbrooke, Département d’informatique, Faculté des Sciences, 2500 Boul. de l’Université, Sherbrooke, QC, Canada, J1K-2R1, pierre-marc.jodoin@usherbrooke.ca

V. Saligrama and J. Konrad are with Boston University, Department of Electrical and Computer Engineering, 8 Saint Mary’s St., Boston, MA 02215 ([srv,jkonrad]@bu.edu)

¹Although models that account for spatial relationships in background subtraction are known, their discussion is beyond the scope of this paper.

This paper is organized as follows. In Section II, we review previous work. In Section III, we recall background subtraction and introduce notation. In Section IV, we introduce behavior space and the notion of an event, while in Section V we describe the behavior subtraction framework. In Section VI, we discuss our experimental results and in Section VII we draw conclusions.

II. PREVIOUS WORK

There are two fundamental approaches to anomaly detection. One approach is to explicitly model all anomalies of interest, thus constructing a dictionary of anomalies, and for each observed video to check if a match in the dictionary can be found. This is a typical case of classification, and requires that *all* anomaly types be known *a priori*. Although feasible in very constrained scenarios, such as detecting people carrying boxes/suitcases/handbags [?], detecting abandoned objects [?] or identifying specific crowd behavior anomalies [?], in general this approach is not practical for its inability to deal with unknown anomalies.

An alternative approach is to model normality and then detect deviations from it. In this case, no dictionary of anomalies is needed but defining and modeling what constitutes normality is a very difficult task. One way of dealing with this difficulty is by applying machine learning that automatically models normal activity based on some training video. Then, any monitored activity different from the normal pattern is labeled as anomaly. A number of methods have been developed that apply learning to two-dimensional motion paths resulting from tracking of objects or people [?]. Typically, the approach is implemented in two steps. In the first step, a large number of “normal” individuals or objects are tracked over time. The resulting paths are then summarized by a set of motion trajectories, often translated into a symbolic representation of the background activity. In the second step, new paths are extracted from the monitored video and compared to those computed in the training phase.

Whether one models anomaly or normality, the background activity must be somehow captured. One common approach is through graphical state-based representations, such as hidden Markov models or Bayesian networks [?], [?], [?], [?], [?]. To the best of our knowledge Johnson and Hogg [?] were the first to consider human trajectories in this context. The method begins by vector-quantizing tracks and clustering the result into a predetermined number of PDFs using a neural network. Based on the training data, the method predicts trajectory of a pedestrian and decides if it is anomalous or not. This approach was subsequently improved by simplifying the training step [?] and embedding it into a hierarchical structure based on co-occurrence statistics [?]. More recently, Saleemi *et al.* [?] proposed a stochastic, non-parametric method for modeling scene tracks. The authors claim that the use of predicted trajectories and tracking method robust to occlusions jointly permit the analysis of more general scenes, unlike other methods that are limited to roads and walkways.

Although there are advantages to using paths as motion features, there are clear disadvantages as well. First, tracking

is a difficult task, especially in real time. Since the anomaly detection is directly related to the quality of tracking, a tracking error will inevitably bias the detection step. Secondly, since each individual or object monitored is related to a single path, it is hard to deal with people occluding each other. For this reason, path-based methods aren’t well suited to highly-cluttered environments.

Recently, a number of anomaly detection methods have been proposed that do not use tracking. These methods work at pixel level and use either motion vectors [?], [?], [?] or motion labels [?], [?], [?] to describe activity in the scene. They all store motion features in an image-like 2D structure (be it probabilistic or not) thus easing memory and CPU requirements. For example, Xiang *et al.* [?] represent moving objects by their position, size, temporal gradient and the so-called “pixel history change” (PHC) image that accumulates temporal intensity differences. During the training phase, an EM-based algorithm is used to cluster the moving blobs, while at run-time each moving object is compared to the pre-calculated clusters. The outlying objects are labeled as anomalous. Although the concept of PHC image is somewhat similar to the behavior image proposed here, Xiang *et al.* do not use it for anomaly detection but for identification of regions of interest to be further processed.

A somewhat different approach using spatio-temporal intensity correlation has been proposed by Shechtman and Irani [?]. Here, an observed sequence is built from spatio-temporal segments extracted from a training sequence. In this analysis-by-synthesis method, only regions that can be built from large contiguous chunks of the training data are considered normal.

Our approach falls into the category of methods that model normality and look for outliers, however it is not based on motion paths but on simple pixel attributes instead. Thus, it avoids the pitfalls of tracking while affording explicit modeling of normality at low memory and CPU requirements. Our contributions are as follows. We introduce the concept of an event, or short-term scene dynamics captured over a time window at a specific spatial location in the camera field of view. With each event we associate features, such as size, direction, speed, busy time, color, etc., and propose a probabilistic model based on time-stationary random process. Finally, we develop a simple implementation of this model by using surrogate quantities that allow low-memory and low-CPU implementation.

III. BACKGROUND SUBTRACTION: ANOMALY DETECTION IN PHOTOMETRIC SPACE

We assume in this paper that the monitored video is captured by a fixed camera (no PTZ functionality) that at most undergoes jitter, e.g., due to wind load or other external factors.

Let \vec{I} denote a color video sequence with $\vec{I}_t(\vec{x})$ denoting color attributes (e.g., R, G, B) at specific spatial location \vec{x} and time t . We assume that $\vec{I}_t(\vec{x})$ is spatially sampled on 2-D lattice Λ , i.e., $\vec{x} \in \Lambda \subset \mathbb{R}^2$ is a pixel location. We also assume that it is sampled temporally, i.e., $t = k\Delta t$, $k \in \mathbb{Z}$, where Δt is the temporal sampling period dependent on the frame rate at which the camera operates. For simplicity, we assume $\Delta = 1$ in this paper, i.e., normalized time. We denote by \vec{I}_t a frame, i.e., a restriction of video \vec{I} to specific time t .

In traditional video analysis, color and luminance are pivotal quantities in the processing chain. For example, in background subtraction, the driving engine of many video analysis tasks, the color of the background is assumed either static or stationary. Although simple frame subtraction followed by thresholding may sometimes suffice in the static case, unfortunately it often fails due to acquisition noise or illumination changes. If the background includes spurious motion, such as environmental effects (e.g., rain, snow), fluttering tree leaves, or shimmering water, then determining outliers based on frame differences is insufficient. A significant improvement is obtained by determining outliers based on PDF estimates of features such as color. Assume that P_{RGB} is a joint PDF of the three color components estimated using a 3-D variant of the mixture-of-Gaussians model [?] or the non-parametric model [?] applied to a training video sequence. P_{RGB} can be used to test if a color at specific pixel and time in the monitored video is sufficiently probable, i.e., if $P_{RGB}(\vec{I}_t(\vec{x})) > \tau$, where τ is a scalar threshold, then $\vec{I}_t(\vec{x})$ is likely to be part of the modeled background, otherwise it is deemed moving.

Although the thresholding of a PDF is more effective than the thresholding of frame differences, it is still executed in the space of photometric quantities (color, luminance, etc.), and thus unable to directly account for scene dynamics. However, modeling of background dynamics (activities) in the photometric space is very challenging. We propose an alternative that is both conceptually simple and computationally efficient. First, we remove the photometric component by applying background subtraction and learn the underlying stationary statistical characterization of scene dynamics based on a two-state (moving/static) renewal model. Then, we reliably infer novelty as a departure from the normality.

IV. BEHAVIOR SPACE: FROM FRAMES TO EVENTS

As color and luminance contain little direct information on scene dynamics, we depart from this common representation and adopt motion label as our atomic unit. Let $L_t(\vec{x})$ be a binary random variable embodying the presence of motion ($L = 1$) or its absence ($L = 0$) at position \vec{x} and time t . Let $l_t(\vec{x})$ be a specific realization of $L_t(\vec{x})$ that can be computed by any of the methods discussed in Section III, or by more advanced methods accounting for spatial label correlation [?], [?].

While some of these methods are robust to noise and background activity, such as rain/snow or fluttering leaves, they often require a large amount of memory and are computationally intensive. Since simplicity and computational efficiency are key concerns in our approach, we detect motion by means of a very simple background subtraction method instead, namely

$$l_t(\vec{x}) = |I_t(\vec{x}) - b_t(\vec{x})| > \tau, \quad (1)$$

where τ is a fixed threshold and b_t is the background image computed as follows

$$b_{t+1}(\vec{x}) = (1 - \rho)b_t(\vec{x}) + \rho I_t(\vec{x}) \quad (2)$$

with ρ in the range 0.001-0.01. This linear background update allows to account for long-term changes. Although this method

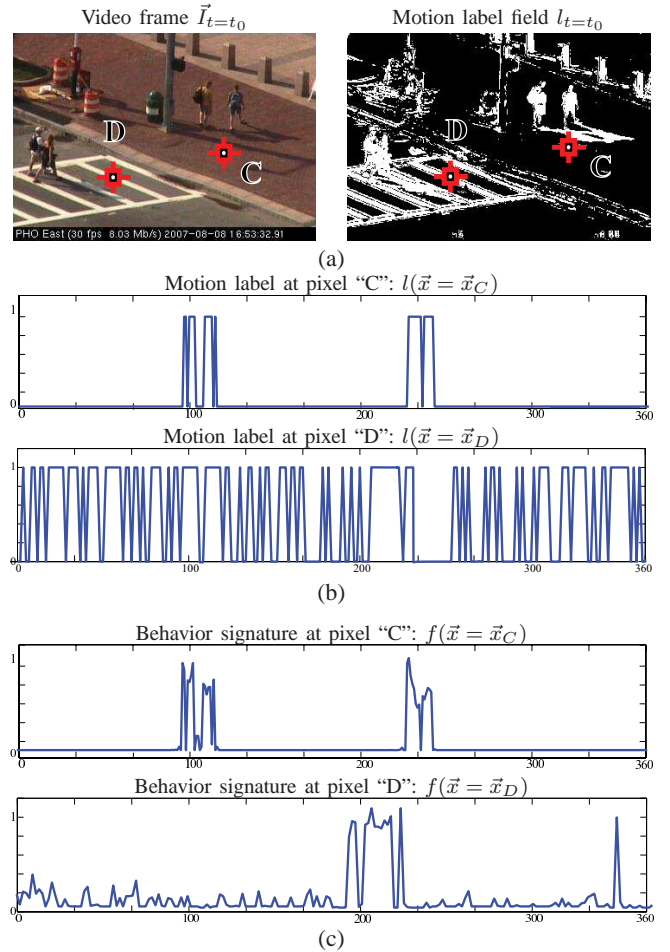


Fig. 1. (a) Video frame $\vec{I}_{t=t_0}$ captured by a vibrating camera and the corresponding motion label field $l_{t=t_0}$. (b) Binary waveforms showing the time evolution of motion labels l at two locations (marked C and D in (a)). (c) Behavior signatures at the same locations computed using the object-size descriptor (3). The pixel located near intensity edge (D) is “busy”, due to camera vibrations, compared to the pixel located in a uniform-intensity area (C). The large bursts of activity in behavior signatures correspond to pedestrians.

is sensitive to noise and background activity, it is trivial to implement, requires very little memory and processing power, and depends on one parameter only. Clearly, replacing this method with any of the advanced techniques will only improve the performance of our approach.

Fig. 1 shows an example realization of motion label field L_t computed by the above method as well as a binary waveform showing temporal evolution of motion label at specific location \vec{x} (Fig. 1.b). Each such waveform captures the amount of activity occurring at a given spatial location during a certain period of time and thus can be considered as a simple *behavior signature*. For instance, patterns associated with random activity (fluttering leaves), periodic activity (highway traffic), bursty activity (sudden vehicle movement after onset of green light), or no activity, all have a specific behavior signature. Other behavior signatures than a simple on/off motion label are possible.

a) *Object descriptor*: A moving object leaves a behavior signature that depends on its features such as size, shape, speed, direction of movement, etc. For example, a large

moving object will leave a wider impulse than a small object (Fig. 1.b), but this impulse will get narrower as the object accelerates. One can combine several features in a descriptor in order to make the behavior signature more unique. In fact, one can even add color/luminance to this descriptor in order to account for photometric properties as well. Thus, one can think of events as spatio-temporal units that describe what type of activity occurs and also what the moving object looks like.

Let a random variable F embody object description², with f being its realization. In this paper, we concentrate on object descriptor based on moving object's size for two reasons. First, we found that despite its simplicity it performs well on a wide range of video material (motor traffic, pedestrians, objects on water, etc.); it seems the moving object size is a sufficiently discriminative characteristic. Secondly, the size descriptor can be efficiently approximated as follows:

$$f_t(\vec{x}) = \frac{1}{N \times N} \sum_{\vec{y} \in \mathcal{N}(\vec{x}); \vec{y} \bowtie \vec{x}} \delta(l_t(\vec{x}), l_t(\vec{y})), \quad (3)$$

where $\mathcal{N}(\vec{x})$ is an $N \times N$ window centered at \vec{x} and $\vec{y} \bowtie \vec{x}$ means that \vec{y} and \vec{x} are connected (are within the same connected component). $\delta(\cdot) = 1$ if and only if $l_t(\vec{x}) = l_t(\vec{y}) = 1$, i.e., if both \vec{x} and \vec{y} are deemed moving, otherwise $\delta(\cdot) = 0$. Note that $f_t(\vec{x}) = 0$ whenever $l_t(\vec{x}) = 0$. This descriptor is zero for a pixel away from the object, increases non-linearly as the pixel moves closer to the object and saturates at 1.0 for pixels inside a large object fully covering the window \mathcal{N} .

Fig. 1.c shows an example of behavior signature based on the size descriptor. Clearly, $f_t(\vec{x}) = 0$ means inactivity while $f_t(\vec{x}) > 0$ means activity caused by a moving object; the larger the object, the larger the $f_t(\vec{x})$ until it saturates at 1. The video frame shown has been captured by a vibrating camera and thus a noisy behavior signature for pixel "D" that is close to an intensity edge.

b) Event model: An event needs to be associated with a time scale. For example, a short time scale is required to capture an illegal U-turn of a car, whereas a long time scale is required to capture a traffic jam. We define an event $E_t(\vec{x})$ for pixel at \vec{x} as the behavior signature (object size, speed, direction as the function of time t) left by moving objects over a w -frame time window, and model it by a Markov model shown in Fig. 2.

For now, consider only the presence/absence of activity (L) as the object descriptor. Assuming π to be the initial busy-state probability ($L = 1$), the probability of sequence $\{L_i = l_i\}_{\mathcal{W}} = (l_{t-w+1}(\vec{x}), l_{t-w+2}(\vec{x}), \dots, l_t(\vec{x}))$, at location \vec{x} and within the time window $\mathcal{W} = [t-w+1, t]$, can be written as follows:

$$\begin{aligned} P_{\vec{x}}(\{L_i = l_i\}_{\mathcal{W}}) &= \pi q^{\beta_1} (1-q) p^{\iota_1} (1-p) q^{\beta_2} (1-q) p^{\iota_2} \dots \\ &= \pi q^{\sum_k \beta_k} p^{\sum_k \iota_k} (1-q)^m (1-p)^n \quad (4) \\ &= \pi (q/p)^{\sum_k \beta_k} p^w (1-q)^m (1-p)^n, \end{aligned}$$

where the binary sequence of 0's and 1's is implicitly expressed through the busy intervals β_k (Fig. 2). Note that m, n are the numbers of transitions "moving \rightarrow static" and "static

² F is a random vector if the descriptor includes multiple features.

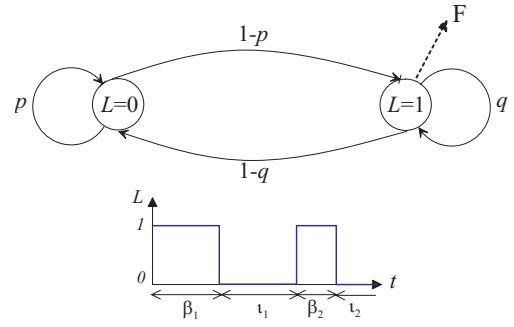


Fig. 2. Markov chain model for dynamic event E : p, q are state probabilities (static and moving, respectively), and $1-p, 1-q$ are transition probabilities. $\beta_1, \iota_1, \beta_2, \iota_2$ denote consecutive busy and idle intervals. With each busy interval is associated an object descriptor F , such as its size, speed/direction of motion, color, luminance, etc.

\rightarrow moving", respectively. The last line in (4) stems from the fact that the sum of busy and idle intervals equals the length of time window \mathcal{W} . This expression can be simplified by taking negative logarithm:

$$\begin{aligned} -\log P_{\vec{x}}(\{L_i = l_i\}_{\mathcal{W}}) &= -\log \pi - (\log q/p) \sum_k \beta_k - w \log p - \\ &\quad m \log(1-q) - n \log(1-p), \quad (5) \\ &= A_0 + A_1 \sum_{k=t-w+1}^t l_k(\vec{x}) + A_2 \kappa_t(\vec{x}), \end{aligned}$$

where A_0, A_1, A_2 are constants, the second term measures the total busy time using motion labels and $\kappa_t(\vec{x})$ is proportional to the total number of transitions in time window \mathcal{W} at \vec{x} .

Thus far we have assumed that the moving object was described only by motion labels $L_t(\vec{x})$. Suppose now that also a descriptor $F_t(\vec{x})$, such as the size, is associated with the moving object at location \vec{x} and time t within a busy period in time window \mathcal{W} , i.e., $t \in \beta_k \subset \mathcal{W}$. The random variable (vector) $F_t(\vec{x})$ is described by a conditional distribution dependent on the state of the Markov process, as illustrated in Fig. 2. We assume that $F_t(\vec{x})$ is conditionally independent of other random variables $F_{t_0}(\vec{x}), t_0 \neq t$ when conditioned on the underlying state of the Markov process, and that its distribution has exponential form when busy and point mass when idle:

$$P_{\vec{x}}(F_t = f_t | L_t = k) = \begin{cases} \frac{1}{Z_1} e^{-A_3 f_t(\vec{x})}, & k = 1, \\ \delta(0), & k = 0. \end{cases} \quad (6)$$

where Z_1 is a partition function and δ is the Kronecker delta. If the descriptor F includes object size, the above distribution suggests that the larger the object passing through \vec{x} the less likely it is, and also that with probability 1 it has size zero in idle intervals (consistent with Fig. 2). This is motivated by the observation that small-size detections are usually associated with false positives when computing L_t . Should F include speed, faster objects would be less likely, a realistic assumption in urban setting. The model would have to be modified should the descriptor include direction of motion (e.g., horizontal motion more likely for highway surveillance with a suitably-oriented camera) or luminance/color (e.g., all photometric properties equally likely).

Note that more advanced descriptor models can be incorporated as well. For instance, one can enforce temporal smoothness of the descriptor (e.g., size) for object passing through location \vec{x} via a (temporal) Gibbs distribution with 2-element cliques:

$$P_{\vec{x}}(\{F_i = f_i\}_{\mathcal{W}} \mid L = 1) = \frac{1}{Z_2} e^{-A_4 \sum_{k: \beta_k \subset \mathcal{W}} \sum_{(j, j+1) \in \beta_k} f_j(\vec{x}) f_{j+1}(\vec{x})},$$

where $\{F_i = f_i\}_{\mathcal{W}}$ denotes a sequence of descriptors appearing in the temporal window \mathcal{W} , and A_4 is a constant. This model controls temporal smoothness of the descriptor F , and can be used to limit, for example, size variations in time. Nevertheless, for simplicity we omit this model in our further developments.

Combining the descriptor model (6) with the L -based event model (4-5) leads to a joint distribution:

$$P_{\vec{x}}(\{L_i = l_i\}_{\mathcal{W}}, \{F_i = f_i\}_{\mathcal{W}}) = P_{\vec{x}}(\{F_i = f_i\}_{\mathcal{W}} \mid \{L_i = l_i\}_{\mathcal{W}}) \cdot P_{\vec{x}}(\{L_i = l_i\}_{\mathcal{W}}) = (7) \prod_{i \in \mathcal{W}} P_{\vec{x}}(F_i = f_i \mid L_i = l_i) \cdot P_{\vec{x}}(\{L_i = l_i\}_{\mathcal{W}})$$

where the last line stems from the conditional independence of F_i 's when conditioned on L 's assumed earlier. Taking the negative logarithm and using equations (5) and (6) results in:

$$-\log P_{\vec{x}}(\{L_i = l_i\}_{\mathcal{W}}, \{F_i = f_i\}_{\mathcal{W}}) = A'_0 + (8) A_1 \sum_{k=t-w+1}^t l_k(\vec{x}) + A_2 \kappa_t(\vec{x}) + A_3 \sum_{k=t-w+1}^t f_k(\vec{x}) l_k(\vec{x}),$$

where A'_0 accounts for Z_1 (6) and the last term is the sum of descriptors in all busy periods in \mathcal{W} . Note that the constant A_2 is positive, thus reducing the probability when frequent "moving \rightarrow static" and "static \rightarrow moving" transitions take place. The constant A_1 may be negative or positive depending on the particular values of q and p in the Markov model; increasing busy periods within \mathcal{W} will lead to an increased ($q > p$) or decreased ($q < p$) joint probability.

Note that at each location \vec{x} the above model implicitly assumes independence among the busy and idle periods as well as conditional independence of F_t when conditioned on $L_t = l_t$. This assumption is reasonable since different busy periods at a pixel correspond to different objects while different idle periods correspond to temporal distances between different objects. Typically, these are all independent³.

With each time t and position \vec{x} we associate an event E_t that represents the statistic described in (8), namely,

$$E_t(\vec{x}) = \sum_{k=t-w+1}^t (A_1 l_k(\vec{x}) + A_3 f_k(\vec{x}) l_k(\vec{x})) + A_2 \kappa_t(\vec{x}), \quad (9)$$

where the constant A'_0 was omitted as it does not contribute to the characterization of dynamic behavior (identical value across all \vec{x} and t) and \mathcal{K} is a random variable associated with realization κ (number of transitions). The main implication of the above event description is that it serves as a sufficient statistic for determining optimal decision rules [?].

³We have performed extensive experiments ranging from highway traffic to urban scenarios and the results appear to be consistent with these assumptions.

c) Anomaly Detection Problem: We first describe anomaly detection abstractly. We are given data, $\omega \in \Omega \subset \mathbb{R}^d$. The nominal data are sampled from a multivariate density $g_0(\cdot)$ supported on the compact set Ω . Anomaly detection [?] can be formulated as a composite hypothesis testing problem. Suppose the test data, ω , come from a mixture distribution, namely, $f(\cdot) = (1 - \xi)g_0(\cdot) + \xi g_1(\cdot)$ where $g_1(\cdot)$ is also supported on Ω . Anomaly detection involves testing the following nominal hypothesis

$H_0 : \xi = 0$ versus the alternative (anomaly) $H_1 : \xi > 0$.

The goal is to maximize the detection power subject to false alarm level α , namely, $\text{Prob}(\text{declare } H_1 \mid H_0) \leq \alpha$. Since the mixing density is unknown, it is usually assumed to be uniform. In this case the optimal uniformly most powerful test (over all values of ξ) amounts to thresholding the nominal density [?]. We choose a threshold $\tau(\alpha)$ and declare the observation, ω , as an outlier according to the following log-likelihood test:

$$-\log(g_0(\omega)) \underset{H_0}{\overset{H_1}{>}} \tau(\alpha) \quad (10)$$

where $\tau(\alpha)$ is chosen to ensure that the false alarm probability is smaller than α . It follows that such a choice is the uniformly most powerful decision rule. Now the main problem that arises is that $g_0(\cdot)$ is unknown and has to be learned in some way from the data. The issue is that ω could be high-dimensional and learning such distributions may not be feasible. This is further compounded in video processing by the fact that it is even unclear what ω , i.e., the features, should be.

It is worth reflecting how we have addressed these issues through our specific setup. We are given w video frames, $I_{t-w+1}, I_{t-w+2}, \dots, I_t$ and a specific location \vec{x} , and our task is to determine whether this sequence is consistent with nominal activity or, alternatively, it is anomalous. We also have training data that describes the nominal activity. In this context, our Markovian model provides a representation for the observed video frames. This representation admits a natural factorization, wherein increasingly complex features can be incorporated, for example through Markov-Gibbs models. Furthermore, the log-likelihood is shown to be reduced to a scalar sufficient statistic, which is parameterized by a finite set of parameters (A_j 's in (9)). Consequently, the issue of learning high-dimensional distribution is circumvented and one is left with estimating the finite number of parameters, which can be done efficiently using standard regression techniques. The problem of anomaly detection now reduces to thresholding the event $E_t = e_t$ according to (10):

$$e_t(\vec{x}) \underset{H_0}{\overset{H_1}{>}} \tau(\alpha),$$

or, explicitly,

$$\sum_{k=t-w+1}^t (A_1 l_k(\vec{x}) + A_3 f_k(\vec{x}) l_k(\vec{x})) + A_2 \kappa_t(\vec{x}) \underset{H_0}{\overset{H_1}{>}} \tau(\alpha). \quad (11)$$

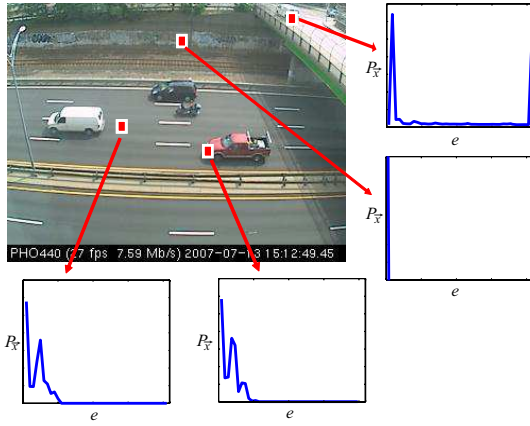


Fig. 3. Event model PDF estimated for four different pixels. The two pixels in traffic lanes have similar histograms due to the fact that their behaviors are very similar (continuous highway traffic). The pixel above the traffic is in the idle area of the video, so its histogram has a high peak near zero, the pixel on the overpass has a bimodal distribution caused by the traffic light.

Our task is to find an appropriate threshold $\tau(\alpha)$ so that the false alarms are bounded by α . Note that our events are now scalar and learning the density function of a 1-D random variable can be done efficiently. The main requirement is that $E_t(\vec{x})$ be a stationary ergodic stochastic process, which will ensure that the CDF can be accurately estimated:

$$\frac{1}{w} \sum_{k=t-w+1}^t \mathbb{I}_{\{E_t(\vec{x}) \geq \eta\}}(e_t(\vec{x})) \rightarrow \text{Prob}_{\vec{x}}\{E \geq \eta\},$$

where $\mathbb{I}_{\{E_t(\vec{x}) \geq \eta\}}(e_t(\vec{x}))$ is an indicator function, equal to 1 when $e_t(\vec{x}) > \eta$ and 0 otherwise, while $\text{Prob}_{\vec{x}}$ denotes the representative stationary distribution for E_t at any time t . For Markovian processes this type of ergodicity is standard [?]. One extreme situation is to choose a threshold that ensures zero false alarms. This corresponds to choosing $\tau(0) = \max_t e_t$, i.e., the maximum value of the support of all events in the training data.

Although the anomaly detection algorithm we describe in the next section requires no explicit estimation of the above CDF, it is nevertheless instructive to understand its properties. Fig. 3 shows example PDFs for our test statistic $e_t(x)$ estimated from training data using smoothed histograms. Note different histogram shapes depending on the nature of local activity.

V. BEHAVIOR SUBTRACTION FRAMEWORK

In the previous section, we presented object and event models, and explained how they fit into the problem of anomaly detection. In principle, once the event model is known various statistical techniques can be applied but this would require significant memory commitment and computational resources. Below, we propose an alternative that is memory-light and processor-fast and yet produces very convincing results.

A. Behavior Images

As mentioned in the previous section, one extreme situation in anomaly detection is to ensure zero false alarms. This requires a suitable threshold, namely $\tau(0) = \max_t e_t$, equal to

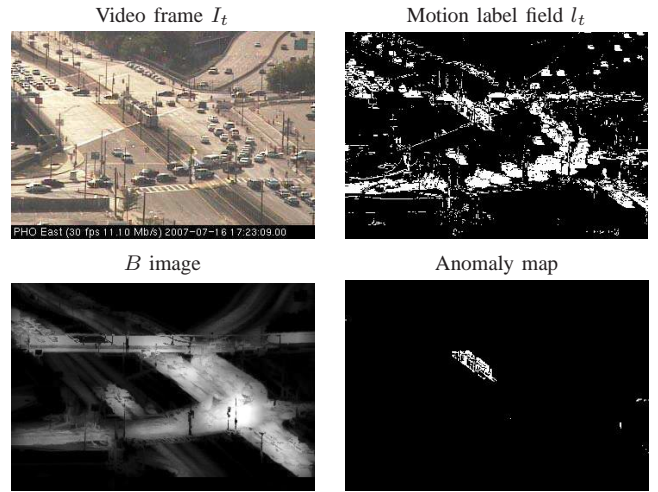


Fig. 4. Behavior subtraction results for the maximum-activity surrogate (12) on data captured by a stationary, although vibrating, camera. This is a highly-cluttered intersection of two streets and interstate highway. Although the jitter induces false positives during background subtraction (L_t), only the tramway is detected by behavior subtraction; the rest of the scene is considered normal.

the maximum value of the support of all events in the training data. This threshold is space-variant and can be captured by a 2-D array:

$$B(\vec{x}) = \max_{t \in [1, M]} e_t(\vec{x}), \quad (12)$$

where M is the length of the training sequence. We call B the *background behavior image* [?] as it captures the background activity (in the training data) in a low-dimensional representation (one scalar per location \vec{x}). This specific B image captures peak activity in the training sequence, and can be efficiently computed as it requires no estimation of the event PDF; maximum activity is employed as a surrogate for normality.

As shown in Fig. 4, the B image succinctly synthesizes the ongoing activity in a training sequence, here a busy urban intersection at peak hour. It implicitly includes the paths followed by moving objects as well as the amount of activity registered at every point in the training sequence.

The event model (9) is based on binary random variables L whose realizations l are computed, for example, using background subtraction. Since the computed labels l will be necessarily noisy, i.e., will include false positives and misses, a positive bias will be introduced into the event model (even if the noise process is *iid*, its mean is positive since labels l are either 0 or 1). The simplest method of noise suppression is by means of lowpass filtering. Thus, in scenarios with severe event noise (e.g., unstable camera, unreliable background subtraction) instead of seeking zero false-alarm rate we opt for event-noise suppression using a simple averaging filter to compute the background behavior image [?]:

$$B(\vec{x}) = \frac{1}{M} \sum_{t=1}^M e_t(\vec{x}). \quad (13)$$

This background behavior image estimates a space-variant bias from the training data. A non-zero bias can be considered as a temporal stationarity, and therefore normality, against which observed data can be compared.

B. Behavior Subtraction

Having defined the zero-false-alarm threshold $\tau(0)$ or event-noise bias *via* the background behavior image B (12-13), we can now apply the event hypothesis test (11) as follows:

$$e_t(\vec{x}) - B(\vec{x}) \underset{\text{normal}}{\overset{\text{abnormal}}{>}} \Theta$$

where Θ is a user-selectable constant allowing for non-zero tolerance ($\Theta = 0$ leads to a strict test). In analogy to calling B a background behavior image, we call e_t an *observed behavior image* as it captures events observed in the field of view of the camera over a window of w video frames. The above test requires the accumulation of motion labels l , object sizes f , and state transitions (κ_t) over w frames. All these quantities can be easily and efficiently computed.

Clearly, abnormal behavior detection in this case simplifies to the subtraction of the background behavior image B , containing an aggregate of long-term activity in the training sequence, from the observed behavior image e_t , containing a snapshot of activity just prior to time t , and subsequent thresholding. This explains the name *behavior subtraction* that we gave to this method.

VI. EXPERIMENTAL RESULTS

We tested our behavior subtraction algorithm for both the maximum- and average-activity surrogates on black-and-white and color, indoor and outdoor, urban and natural-environment video sequences. In all cases, we computed the label fields l_t using simple background subtraction (1) with $\tau = 40$ and background b updated with α between 10^{-3} and 10^{-2} , depending on the sequence. Although we have performed experiments on a wide range of model parameters, we are presenting here the results for event model based on size descriptor (3) ($A_1 = A_2 = 0$).

The results of behavior subtraction using the maximum-activity surrogate (12) are shown in Figs. 4-???. Each result was obtained using a training sequence of length $M=1000$ -5000 frames, $w = 100$, and $\Theta \in [0.5, 0.7]$. As is clear from the figures, the proposed method is robust to inaccuracies in motion labels l_t . Even if moving objects are not precisely detected, the resulting anomaly map is surprisingly precise. This is especially striking in Fig. 4 where a highly-cluttered environment results in high density of motion labels while camera jitter corrupts many of those labels.

Behavior subtraction is also effective in removal of unstructured, parasitic motion such as due to water activity (fountain, rain, shimmering surface), as illustrated in Fig. 5. Note that although motion label fields l_t include unstructured detections due to water droplets, only the excessive motion is captured by the anomaly maps (passenger car and truck with trailer). Similarly, the shimmering water surface is removed by behavior subtraction producing a fairly clean boat outline in this difficult scenario. Our method also manages to detect abandoned objects and people lingering, as seen in the two bottom rows of Fig. 5.

Fig. ?? shows yet another interesting outcome of behavior subtraction. In this case the background behavior image

was trained on a video with single pedestrian and fluttering leaves. While the object-size descriptor captures both individual pedestrians and groups thereof, anomalies are detected only when a large group of pedestrians passes in front of the camera.

The results of behavior subtraction using the average-activity surrogate are shown in Fig. ???. The video sequence has been captured by a vibrating camera (structural vibrations of camera mount). It is clear that behavior subtraction with average-activity surrogate outperforms background subtraction based on single-Gaussian model [?] and non-parametric-kernel model [?]. As can be seen, behavior subtraction effectively eliminates false positives without significantly increasing misses.

As already mentioned, the proposed method is efficient in terms of processing power and memory use, and thus can be implemented on modest-power processors (e.g., embedded architectures). For each pixel, it requires one floating-point number for each pixel of B and e , and $w/8$ bytes for l . This corresponds to a total of 11 bytes per pixel for $w = 24$. This is significantly less than 12 floating-point numbers per pixel needed by a tri-variate Gaussian for color video data (3 floating-point numbers for R, G, B means and 9 numbers for covariance matrix). Our method currently runs in *Matlab* at 20 fps on 352×240 -pixel video using a 2.1 GHz dual-core Intel processor. More experimental results can be found in our preliminary work [?], [?], while complete video sequences can be downloaded from www.dmi.usherb.ca/~jodoin/projects/PAMI2009.

VII. CONCLUSIONS

In this paper, we proposed a framework for the characterization of dynamic events and, more generally, behavior. We defined events as spatio-temporal signatures composed of various moving-object features, and modeled them using stationary random processes. We also proposed a computationally-efficient implementation of the proposed models, called behavior subtraction. In fact, due to simple surrogates of activity/behavior statistics used, behavior subtraction is very easy to implement, uses little memory and can run on an embedded architecture. Furthermore, the proposed framework is content-blind, i.e., equally applicable to pedestrians, motor vehicles or animals. Among applications that can benefit from the proposed framework are suspicious behavior detection and motion detection in presence of strong parasitic background motion. Yet, challenges remain. One challenge is to extend the proposed concepts to multiple cameras so that a mutual reinforcement of decisions takes place; some of our preliminary work can be found in [?]. Another challenge is to detect anomalies at object level while using only pixel-level decisions proposed here.

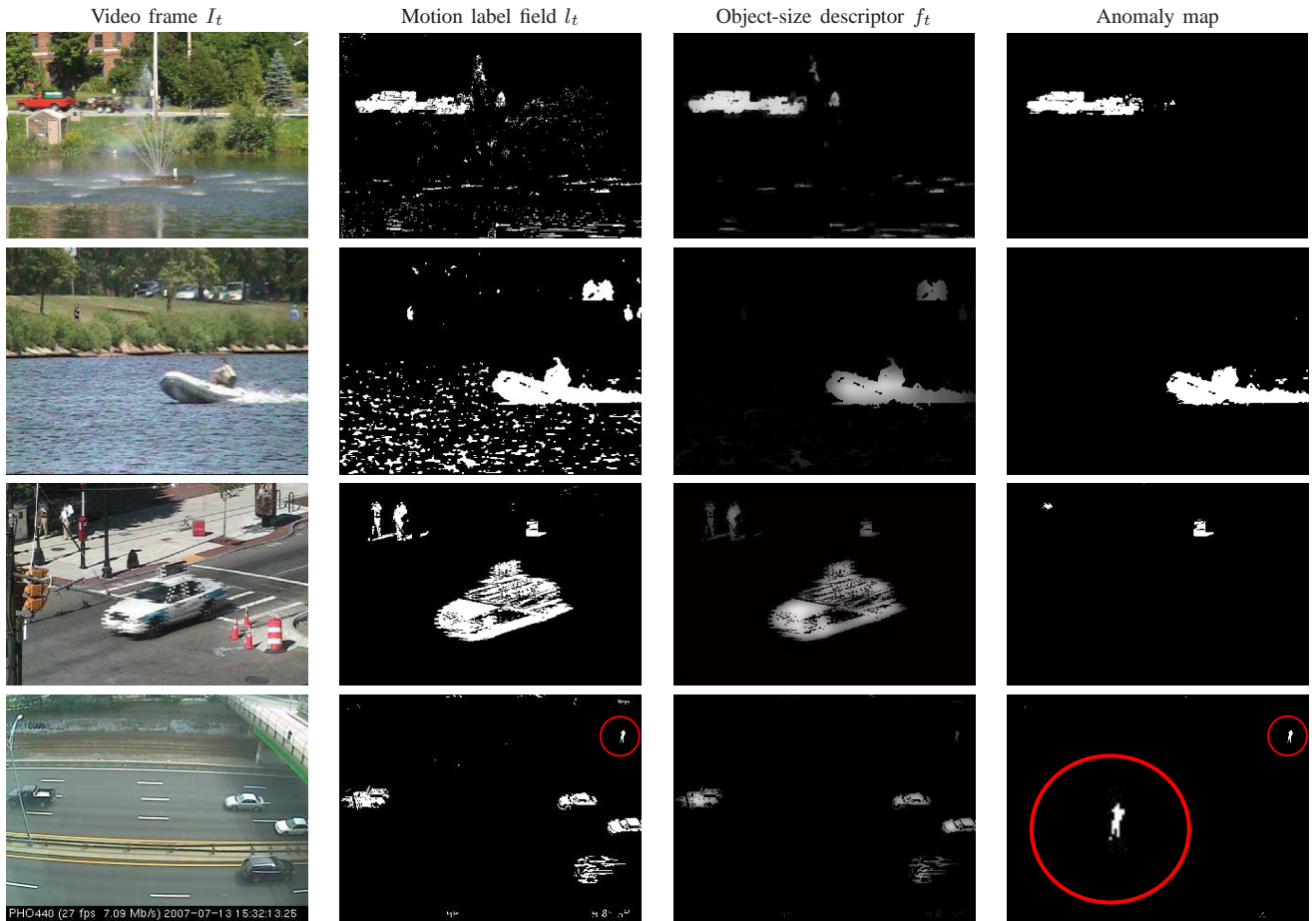


Fig. 5. Behavior subtraction results for maximum-activity surrogate (12) on video sequences containing shimmering water surface (two top rows), strong shadows (third row) and very small abnormally-behaving object (bottom row).